Electric Field DC Conductivity Dependency of Polyimide Films

Luke Guinane and **Syed A.M. Tofail**
University of Limerick
Bernal Institute
Limerick, Ireland

Bernard Stenson, John O'Malley, Colm Glynn and **Shane Geary**
Analog Devices International
Limerick, Ireland

Sombel Diaham
LAPLACE
Université de Toulouse, CNRS
Toulouse, France

ABSTRACT

The isolation behaviour of polyimide thin films has been studied. Properties such as DC conductivity and the threshold electrical fields were obtained through a steady state current measurement under an applied voltage across a metal-insulator-metal capacitor. An inverse relationship has been found between the curing temperature and threshold electric field that would be applied to the structure. The results correlate with high voltage endurance life-time curves for digital isolators processed at different temperatures.

Index Terms — **polyimide, cure temperature, threshold field, breakdown, DC conductivity**

1 INTRODUCTION

ISOLATORS are electronic devices that transmit digital signals to and from controllers whilst also providing galvanic isolation to deliver safe voltage levels for user interfaces and low voltage circuitry. They have a wide range of applications including industrial, automotive, consumer and medical electronics, each requiring a specific minimum level of isolation. The basic forms of isolation are provided by optical, capacitive and magnetic coupling [1]. An isolator must pass several regulatory standards before it can be released to the marketplace. These include reliability tests such as withstand and surge voltage as well as high voltage endurance (HVE). Withstand and surge voltage are relatively quick duration tests, however, HVE may take several months to years to complete [2]. The present work is based on the evaluation of the isolation capabilities of materials used in magnetically coupled isolators. To better manage reliability testing of isolators, it is ideal to optimise the component materials beforehand. In this work we discuss the influence of processing effects on various materials used in isolators and their behaviour prior to electrical breakdown. Polyimide (PI) is an electrical insulator widely used in microelectronic devices due to its desirable electrical properties and ease of processing. PI is thermally, chemically and mechanically stable reinforcing its suitability to microelectronics [3]. The isolation properties of PI are affected by several variables including thickness, area, process methods, interfacial electrodes and environmental conditions such as temperature and humidity [4–9].

Here, we report the electrical properties of PI with a targeted thickness of 10 μm subject to different curing temperatures. The influence of humidity is also reported.

2 EXPERIMENTAL DETAILS

2.1 SAMPLE PREPARATION

To determine electrical properties of PI, metal-insulator-metal (MIM) capacitor structures similar to that reported in [10] were fabricated. The MIM capacitor was processed in a cleanroom. The MIM capacitor is based on 4 functional layers deposited and patterned onto a silicon (Si) substrate. Figure 1 highlights the major processing steps of the samples. The first layer was 400 nm of AlSiCu. It is sputter deposited and will

Manuscript received on 17 February 2020, in final form 3 June 2020, accepted 8 June 2020. Corresponding author: L Guinane.

DOI: 10.1109/TDEI.2020.008861

act as the HV electrode. A 200 nm oxide and 700 nm nitride films were then deposited for a passivation over the HV electrode as shown in Figure 1a.

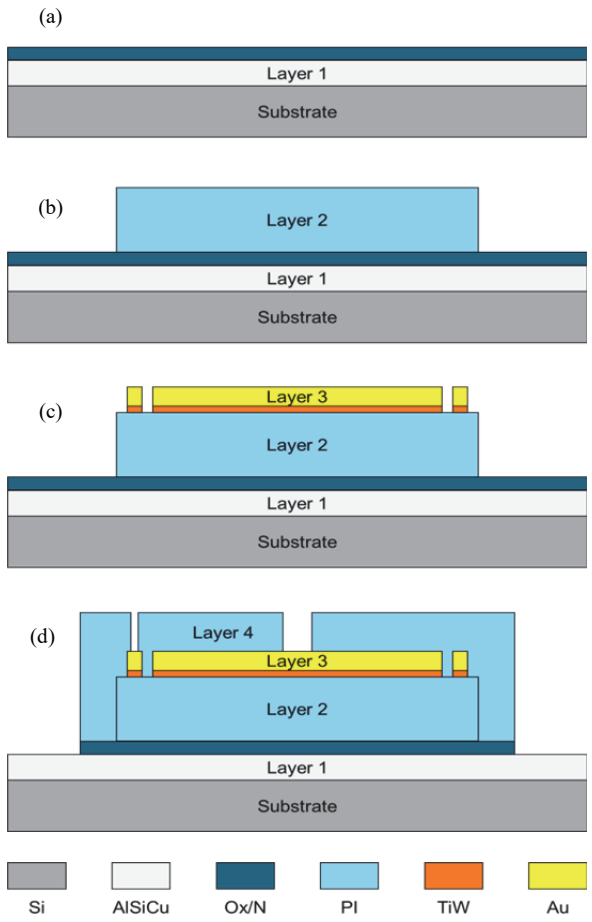

Figure 1. Deposition of key layers in a MIM capacitor. (a) Layer 1 is the bottom electrode. (b) Layer 2 is the PI layer under investigation. (c) Layer 3 is the disc electrode and guard ring. (d) Layer 4 is a protective PI layer.

The second layer was PI with a thickness of 10 µm shown in Figure 1b. A PI precursor was spin coated onto the surface of the wafer, then photo-exposed, developed and thermally cured appropriately. This was the main layer under investigation in the experiments. The area of the PI was 22 x 22 mm^2. The third layer is 6 µm of gold (Au). It was deposited by electroplating on a TiW/Au seed layer covered in a patterned photo resist. The plated areas formed a disc electrode, 17 mm in diameter and a guard ring with an outer and inner diameter of 19 mm and 18 mm respectively. The resulting width of the guard ring was 0.5 mm. The disc was used to measure leakage current through the PI film. The fully deposited guard ring and disc electrode are shown in Figure 1c. The final functional layer, layer 4, was an additional PI film. It was spin coated, exposed, developed and cured to provide contact with the guard ring and disc electrodes. This layer provided safety during measurement and was to reduce the probability of arcing and breakdown under high field from the top Au electrode, guard ring and the bottom AlSiCu electrode. The final process step used an ion beam etch to remove the 200 nm oxide and 700 nm nitride passivation layer that covered the bottom HV electrode. The removed oxide, nitride and layer 4 are shown in Figure 1d. Once fully processed, the wafer was diced into an area of 30 x 30 mm^2.

2.2 ELECTRICAL SETUP

The electrical properties of the PI were extracted using a home built current-voltage (I-V) test system. A Signatone S-1160 probe station was setup in a Faraday cage to negate the influence of external electric fields. An aluminium nitride slate was placed on the stage and the sample was placed on this slate. The electrical circuit of the system is shown in Figure 2. The DC voltage was supplied by a 6.5 kV source which was connected to the AlSiCu electrode and the guard ring. A Keithley 6517A electrometer measured the leakage current flowing from the AlSiCu electrode to the Au disc. The electrometer had a resolution of 0.5 pA. A LabVIEW program recorded the leakage current as a function of time.

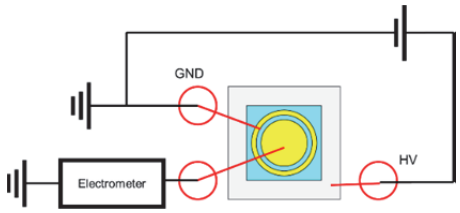

Figure 2. Probe station setup. The power source is connected to the AlSiCu substrate and the ground ring. The disc electrode is connected to a Keithley 6517A electrometer/high resistance meter.

The high voltage was applied to the MIM capacitor for 30 minutes as the current reached a steady state. After this, the voltage was reduced to zero. As PI can store charge [11], the sample was left to discharge for a further 30 minutes. It may take several hours to days for a sample to fully discharge as mentioned in [12]. Low field excitation takes a relatively short duration to reach a steady state current. As the field strength increases, this duration will increase. We have chosen a fair compromise of 30 minutes with an aim to get a complete set of measurements within a single day. We expect, the measured steady state values, even if slightly overestimated to be in good agreement with the literature [13]. After the sample was discharged, the voltage was increased, as shown in Figure 3. To account for environmental parameters, half of the samples were placed in an oven at 150 ^{o}C for 48 hours to remove moisture

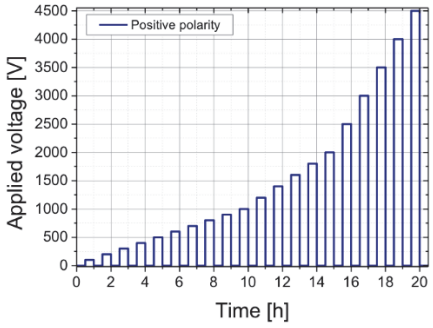

Figure 3. Voltage cycling for MIM capacitor under investigations. The voltage is applied for 30 minutes and then switched off for an additional 30 minutes to allow the sample to discharge.

from the PI layers. Other studies on thin film PI have removed moisture from the films with temperatures in excess of 150 °C which did not degrade or alter the properties of the PI [14,15]. The drying process aids in the removal of homo charges that would be present in the PI near the electrodes. All measurements were carried out at room temperature.

2.3 POLYIMIDE THICKNESS

The electric field across the electrodes of the MIM capacitor is dependent on the thickness of the PI film. The targeted PI thickness is 10 µm. However, it is reported that the thickness of PI films varies during processing steps. In particular, the curing step will alter the PI thickness as solvents are removed and imidization occurs. The imidization forms closed imide rings in the PI precursor, ultimately reducing the thickness of the final PI under investigation [16]. The amount of imidization and solvent removed will depend on the curing time and temperature. To verify the electric field across the MIM capacitor, the thickness of the PI layers was measured by a cross-sectional focused ion beam (FIB). A gallium ion source etched away a section of the MIM capacitor. The cross-section was then observed with a scanning electron microscope. Next the thickness of the PI film under investigation was measured.

3 RESULTS AND DISCUSSION

3.1 STEADY STATE CURRENT

Figures 4a and 4b shows the results of charging current versus time when voltage is applied to the sample for different PI cure temperatures. The MIM capacitors displayed similar current versus time plots up to an applied voltage of 1000 V. Above this voltage, the MIM capacitor with PI cured at a higher temperature had a larger charging current for an equivalent applied voltage compared to the lower cure temperature. Additionally, the current decay was slower. The slower decay was expected to be due to the slow filling of trap sites in the PI [11]. The lower cure temperature sample also exhibited this behaviour but at larger voltages. In Figure 4b, after 1000 s, the charging current exhibited a peak. Similar charging current phenomena has been observed in the literature due to the formation of space charge [17]. Eventually, the higher cure temperature MIM capacitor suffered electrical breakdown at 3500 V after 1000s. The current at this voltage was also increasing with time due to space charge injection.

3.2 ISOLATION PROPERTIES

To extract properties such as the DC conductivity, σ_{DC}, and threshold electric field, E_{Th}, the thickness of PI for each capacitor was measured by FIB cross-section. The PI films cured at a higher temperature had a lower thickness and the PI films cured at a lower temperature had a larger thickness. The higher and lower cured temperature PI had an average thickness value of 12.4 and 14.5 µm, respectively. The electric field, E, was obtained by dividing the applied voltage, V_{app} by the PI thickness, d. The current density in the PI film was obtained by dividing the measured solid-state current, I_C, at 30

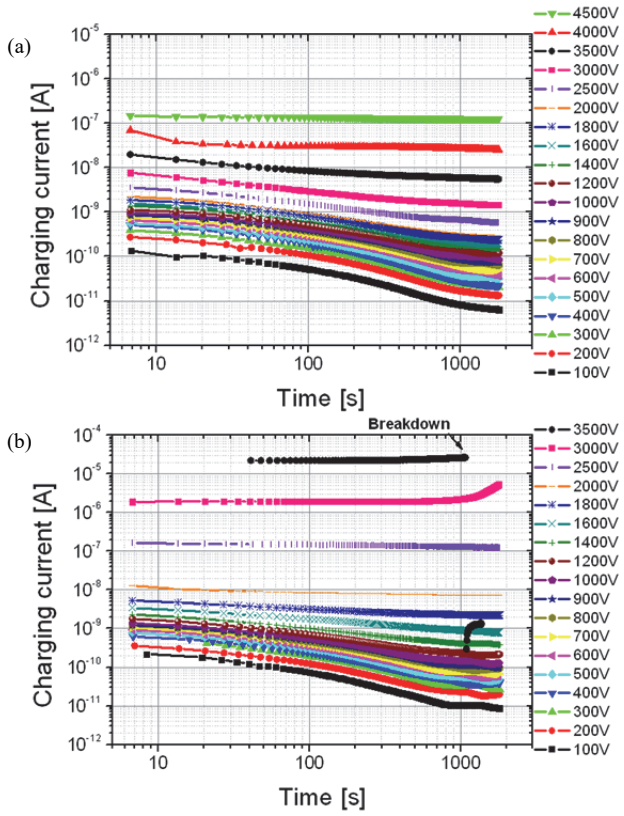

Figure 4. Current vs time for a series of applied voltages. (a) PI cured at a lower temperature. (b) PI cured at a higher temperature.

mins by the gold disc electrode area, S. The DC conductivity was calculated with Equation (1):

$$\sigma_{DC} = \frac{J}{E} = \frac{I_c}{S}\frac{d}{V_{app}} \quad (1)$$

Figures 5a, 5b and 5c shows plots of DC conductivity versus electric field for different parameters. The key findings of the plots are tabulated in Table 1. The estimated dispersion in DC conductivity is expected to be less than 5%.

Figure 5a shows DC conductivity as a function of the applied electric field for the MIM capacitor with a low and high cure temperature. At low fields, both samples had similar values of DC conductivity. The current transferred from one electrode to the other was expected to be ohmic. However, there were notably different threshold fields. Once this field was exceeded, the DC conductivity became a non-linear function of the electric field. As the electric field increased, the slope of the curve also increased. The catalyst for this change was expected to be due to the injection of space charge from the electrode. The presence of the space charge distorts the electric field distribution in the PI, increasing the conductivity, thus aging the PI [18].

The threshold field occurred at a lower field for the higher cured temperature sample than the lower cured sample. The earlier space charge injection appears to have degraded the insulation properties at a quicker rate, ultimately causing the higher cured sample to breakdown. The value of the threshold field was estimated to be the point where the DC conductivity

Table 1. Field independent DC conductivity and threshold electric field for PI cure temperature.

Cure temperature	PI *d* (μm)	Moist or dried	σ_{DC} (S/cm)	E_{TH} (kV/mm)	E_{BD} (kV/mm)
Low	14.5	Dried	~40E-18	~110	-
High	12.4	Dried	~50E-18	~80	~280
Low	14.5	Moist	~30E-15	~10	-
High	12.4	Moist	~20E-15	~30	~280

became non-linear. These values were about 110 and 80 kV/mm for the low and high cure temperatures respectively. Beyond their threshold fields, the slopes of conductivity vs field appeared to become approximately equal again prior to breakdown. The similar slopes indicated that they were undergoing the same conduction mechanism at these values [14]. The higher cure temperature resulted in a thinner PI film and thus a larger electric field for an applied voltage but was not the expected reason for breakdown.

It is expected that the curing temperature altered the insulation capabilities of the film. Thermal curing induces imidization in the PI precursor. When PI is cured at a higher temperature, it increases the degree of imidization. PI is reported to start imidization at 200 °C and is said to imidize fully when curing at 400 °C. The degree of imidization will affect the final properties of fully processed PI [19]. At a higher cure temperature, more of the PI precursor is converted to PI forming more imide rings. A higher cure temperature is expected to reduce the number of defects, but if it is cured at too high a temperature, the PI is likely to degrade. In a PI film, chains may be stacked in such a way that there is a charge transfer complex (CtC) between electron acceptors and donors of two separate chains. The bond formed by CtC is weaker compared to a covalent bond and is affected by the imidization process. Increased imidization, leads to more chains stacked by CtC, creating more possible conduction paths. A higher cure temperature may lead to further stacking and potential conduction paths in the film [20,21].

The effect of moisture on the properties are observed in Figures 5b and 5c. For both the lower and higher cured films, at low fields, the DC conductivity was almost 2 orders greater when moisture was present in the films. The imide bonds in the PI structure are likely to have absorbed the moisture. The water molecule contributes an OH^- molecule that bonds to a carbonyl group and H^+ bonds to amine. This generates ionic side groups in the PI chain which greatly contribute to charge transport in the form of intrinsic ionic conduction [14]. The moisture in the sample also reduces the height of the potential barrier, enabling space charge injection from the electrode [18,22]. As the DC conductivity of both lower and higher cured samples with moisture (undried) were similar at low fields, it seems that they have the same water absorption properties. However, as the samples were subject to increasing field strengths, the response of DC conductivity varied depending on the cure temperature. This behaviour indicates that both the presence of moisture and the cure temperature may alter the conduction mechanism at different fields.

In Figure 5b, for the undried sample, it appeared that the threshold field was exceeded upon the initial excitation as the

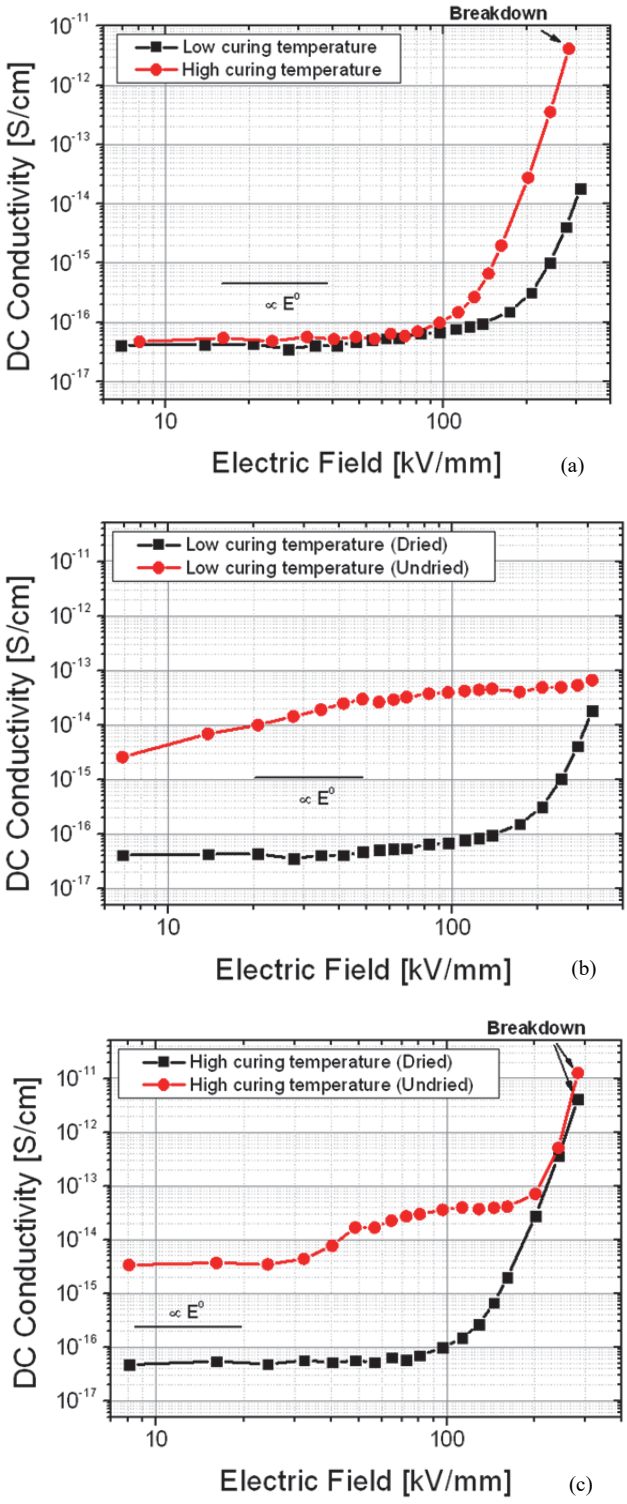

Figure 5. Plots of DC conductivity vs electric field. (a) Comparison of cure temperature. (b) and (c) comparison of undried (moisture present) and dried samples for low and high temperature cure respectively.

conductivity and field relationship was already non-linear. The shape of this curve indicates that the conduction mechanism was already non-ohmic, and the injection of space charge had occurred. The presence of water in the PI was expected to reduce the dielectric constant and trap depth [23]. Additionally, the presence of moisture may have changed the local state and could have contributed to additional hopping sites in the film, affecting conduction [23]. The additional trap sites in this PI film were expected to be shallow with respect to distance from the electrode as they coincide with the apparent flattening of the curve as the conductivity fluctuates slightly as the exciting field increases beyond 50 kV/mm.

Figure 5c, shows the change in DC conductivity for samples cured at a higher temperature with both moisture present (undried) and dried out of the PI. Both the dried sample and undried sample eventually suffered electrical breakdown. After the initial excitation, the DC conductivity appeared to be independent of the field, up to the threshold field around 30 kV/mm. Space charges were expected to enter the PI beyond this point. However, between 50 and 200 kV/mm for the undried sample, the curve slightly flattened out. This section of the curve was expected to involve filling of a trap site introduced by presence of moisture in the film [24]. The trapping mechanism caused a temporarily stall in the increase of the DC conductivity. Upon filling of these traps, beyond 200 kV/mm, the slope increased and eventually breakdown occurred. Above 200 kV/mm, the slopes of the dried and sample with moisture were almost parallel. Here, the parallel nature indicates that they were experiencing the same conduction phenomena from trap sites thought to be intrinsic to the PI due to the curing temperature [14,17]. This steep area of the curve has been reported to dependent on the filling of traps near the electrode [25]

Interestingly, the impact of PI processing temperature appeared to be more significant than the presence of moisture. The MIM capacitor processed at lower temperature did not breakdown when moisture was present in the film even though the low field DC conductivity was nearly two orders larger than a sample with moisture removed. Whereas the MIM capacitor processed at higher temperature did breakdown when moisture was removed from the film. This breakdown field appeared to occur near 280 kV/mm.

4 CONCLUSIONS

The relationship between the insulation capabilities of PI films and processing temperatures and moisture content was investigated by measuring the leakage current in a MIM capacitor using an I-V measurement system. For films approximately 10 µm thick with different cure temperatures, at low fields, their DC conductivities are roughly equal. However, they have different threshold fields. The lower and higher temperature cured PI films had a threshold field about 110 kV/mm and 80 kV/mm respectively. Also, the MIM capacitor cured at the higher temperature eventually suffered electrical breakdown.

Additionally, we found that the polymer processing temperature has more impact on the breakdown voltage than the presence of moisture. Moisture increased the DC conductivity by two orders at low fields, lowered the threshold fields and apparently introduced local shallow trapping sites, but did not necessarily induce breakdown at higher electric fields. The sample cured at a lower temperature subject to moisture didn't breakdown during testing. While the sample cured at a higher temperature suffered electrical breakdown around 280 kV/mm when moisture was removed. We speculate the higher degree of imidization coinciding with a higher cure temperature, increased the effective number of conduction paths in the PI, altering the transport of space charge, increasing the aging of the PI film, leading to an eventual breakdown at higher electric fields.

This study has allowed us to identify parameters which affect the intrinsic failure mechanisms in insulating PI films. The results of our study correlate with HVE measurements. Isolators processed with lower cure temperatures had longer lifetimes than isolators with higher cure temperatures. The I-V measurements took approximately 20 hours to complete per sample. This duration is significantly shorter than standard HVE measurements. This study will be used to optimise the management of isolators undergoing HVE measurements.

ACKNOWLEDGMENT

The authors would like to thank the Irish Research Council (IRC) Enterprise Partnership Scheme (EPS) under the project ID: EBPPG/2016/271. Moreover, the authors thank the European Union and the Marie Skłodowska-Curie Action (MSCA-IF, H2020 program) for financial funding in the frame of the PRISME project (grant N°846455, 2019-2021).

REFERENCES

[1] B. Chen, J. Wynne, and R. Kliger, "High speed digital isolators using microscale on-chip transformers," Elektronik Mag., 2003

[2] D. Krakauer, "Safety Reliability of Digital Isolators," technical article MS-2423, available on www.analog.com, 2012

[3] S. Diaham, M.-L. Locatelli, and T. Lebey, "Conductivity spectroscopy in aromatic polyimide from 200 to 400° C," Appl. Phys. Lett., vol. 91, no. 12, p. 122913, 2007.

[4] S. Diaham *et al*, "Dielectric breakdown of polyimide films: Area, thickness and temperature dependence," IEEE Trans. Dielectr. Electr. Insul., vol. 17, no. 1, pp. 18-27, 2010.

[5] D. Min *et al,* "Thickness-dependent DC electrical breakdown of polyimide modulated by charge transport and molecular displacement," Polymers, vol. 10, no. 9, p. 1012, 2018.

[6] N. Song *et al,* "Decreasing the dielectric constant and water uptake by introducing hydrophobic cross-linked networks into co-polyimide films," Appl. Surface Sci., vol. 480, pp. 990–997, 2019.

[7] Y. Kish *et al*, "Breakdown and space charge formation in polyimide film under DC high stress at various temperatures," *J. Phys. Conf. Series,* 2009, vol. 183, no. 1, p. 012005.

[8] N. Tu and K. Kao, "High-field electrical conduction in polyimide films," J. Appl. Phys., vol. 85, no. 10, pp. 7267-7275, 1999.

[9] M.-L. Locatelli *et al,* "Space charge formation in polyimide films and polyimide/SiO2 double-layer measured by LIMM," IEEE Trans. Dielectr. Electr. Insul., vol. 24, no. 2, pp. 1220–1228, 2017.

[10] S. Diaham and M.-L. Locatelli, "Space-charge-limited currents in polyimide films," Appl. Phys. Lett., vol. 101, no. 24, p. 242905, 2012.

[11] G. G. Raju, R. Shaikh, and S. U. Haq, "Electrical conduction processes in polyimide films-I," IEEE Trans. Dielectr. Electr. Insul., vol. 15, no. 3, pp. 663-670, 2008.

[12] J. Vanderschueren and A. Linkens, "Nature of transient currents in polymers," Journal of Applied Physics, vol. 49, no. 7, pp. 4195–4205.
[13] F. W. Smith *et al*, "Electrical conduction in polyimide between 20 and 350 C," Journal of electronic materials, vol. 16, no. 1, pp. 93–106, 1987.
[14] L. Li, *et al*. "Statistical analysis of electrical breakdown behavior of polyimide following degrading processes," IEEE Trans. Dielectr. Electr. Insul., vol. 18, no. 6, pp. 1955–1962, 2011
[15] K. Kaneko *et al*, "Space charge behavior of polyimide film," Proceedings of the 2004 IEEE International Conference on Solid Dielectrics, vol. 1, pp. 150–153, 2004.
[16] Y. Chen et al, "Fabrication of polyimide sacrificial layers with inclined sidewalls based on reactive ion etching," AIP Advances, vol. 4, no. 3, p. 031328, 2014.
[17] S. Diaham *et al*, "Huge improvements of electrical conduction and dielectric breakdown in polyimide/BN nanocomposites," IEEE Trans. Dielectr. Electr. Insul., vol. 23, no. 5, pp. 2795–2803, 2016.
[18] L. R. Zhou *et al*, "Study on charge transport mechanism and space charge characteristics of polyimide films," IEEE Trans. Dielectr. Electr. Insul., vol. 16, no. 4, pp. 1143–1149, 2009.
[19] S. Diaham *et al*, "Thermal imidization optimization of polyimide thin films using Fourier transform infrared spectroscopy and electrical measurements," Thin Solid Films, vol. 519, no. 6, pp. 1851–1856, 2011.
[20] A. Georgiev *et al, Chemical and physical properties of polyimides: biomedical and engineering applications*, InTech, 2012.
[21] M. Ghosh, *Polyimides: fundamentals and applications*., CRC press, 1996.
[22] S. Fujita and Y. Kamei. "Electrical properties of polyimide with water absorption," IEEE, 11th Int. Symp. Electrets (ISE), 2002, pp. 275–278.
[23] K. Kaneko, *et al,* "Effects of absorbed water on space charge and conduction phenomena in polyimide films," Annu. Rep. Conf. Electr. Insul. Dielect. Phenom. (CEIDP), 2005. pp. 657–660.
[24] Y. Fan *et al*, "The impact of air relative humidity on corona-resistant polyimide film," *IEEE 6th Intern. Forum on Strategic Technology,* 2011. vol. 1, pp. 80–83.
[25] Y. Chen, *et al,* (2017, September). "Study on conduction current characteristics of corona-resistant polyimide film before and after thermal aging," *IEEE Int. Symp. Electr. Insul. Mat. (ISEIM),* 2017, vol. 2, pp. 605–608.